1 Introduction

1.1 Flexible Aircraft Dynamics: Expanding Aircraft Designers' Toolkit

Flexible aircraft dynamics is the study of air vehicles in atmospheric flight that *simultaneously* display both rigid-body and elastic behavior. Since all aircraft deform and vibrate to some extent under aerodynamic forces, we can safely state that all aircraft are flexible. However, for most aircraft currently in operation, airframe flexibility has a negligible effect in the vehicle's flight dynamics, and most of the time, both effects can be independently analyzed. As we argue below, this is unlikely to stay in the next-generation aircraft, and this book presents an analysis framework that enables the rigid and elastic contributions to the aircraft dynamics to be considered at once. While this is of high relevance for both aircraft design and operation, including pilot training, our focus will be on the design phase, and therefore, it is convenient to outline first the stages of the design cycle for a new aircraft. *Appropriate fidelity* models and tools are employed based on the knowledge and information available at that particular stage of the design.

The initial, exploratory phase is known as *conceptual design*. At this stage, target performance requirements for a given mission are selected (for a transport aircraft, they would be metrics like range, payload, and operational cost), and the basic features of an aircraft that would meet them, as well as generic road maps for its commercial and technological viability, are established. In the conceptual design, multiple competing configurations are typically investigated, and the main design trade-offs (e.g., whether the engines should be wing or tail mounted) are analyzed for their sizing. Experimental tests, such as wind-tunnel tests, may be spun out to investigate critical enabling technologies in some detail, but a key feature of this phase is the use of *low-order* models. This phase is followed by the *preliminary design* stage, in which disciplinary analysis is carried out to establish confidence in the viability in the design. Specialist teams from structures, aerodynamics, flight dynamics and control, manufacturing, systems, etc. assess the initial design to identify potential roadblocks, for which they attempt to propose potential solutions. Those disciplinary models produce a first full description of the main components of the aircraft, including its external geometry and key manufacturing and assembly choices. In the last two decades, cross-disciplinary teams have started to appear at this stage to systematically investigate some key trade-offs using multidisciplinary design optimization (MDO) strategies. A successful preliminary design with a plausible business case may result in the full

https://doi.org/10.1017/9781108354868.002 Published online by Cambridge University Press

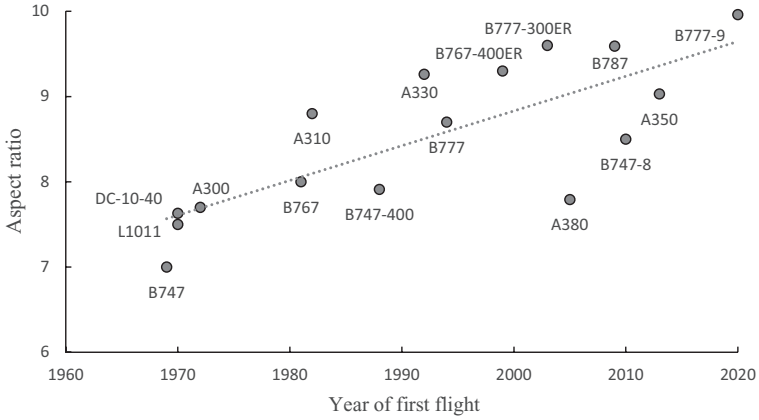

Figure 1.1 Aspect ratio by year of first flight of long-range transport aircraft.

development of the vehicle, and this is done in the final *detail design* phase. Detail design performs all the necessary analysis to manufacture and certify the vehicle, and it is supported by extensive ground-based and in-flight testing of components and full-vehicle prototypes. It is much more complex and costly than the previous two stages, and it stretches over several years.

Design is often described as the art of compromise, and aircraft designers are constantly faced, particularly in conceptual studies, with some fundamental trade-offs. The oldest and arguably most important aircraft design trade-off of all is that between aerodynamic and structural efficiency. Most aircraft are designed using the *tube-and-wing configuration*, which decouples the generation of lift in the wings from the hosting of the payload in the fuselage. This also means that lift is generated in a different part of the aircraft to where it is actually needed (to counteract the weight of passengers and payload, of course), from which the basic layout of their structural design starts to emerge. The historical trend is to improve aerodynamic efficiency while reducing airframe weight, as both directly contribute to an improvement in fuel efficiency. Aerodynamic efficiency is greatly improved by increasing the wing aspect ratio, defined as the ratio of the square of the wingspan over the wing area. However, longer and lighter wings are also necessarily more flexible, and structural considerations put an upper limit to the final wingspan in the design (the second limit comes from ground infrastructure). The maximum aspect ratio considered in aircraft design has steadily increased through the last decades as materials and manufacturing methods have improved. This can be seen in Figure 1.1, which shows the aspect ratio of most modern wide-body airliners against the year of their first flight. Note, however, that very large aircraft, such as the Airbus A380, are constrained in the wingspan by the ground infrastructure, which produces some scattering in the graph (and worse fuel efficiency).

It is interesting to present some numbers here to understand certain underlying design choices. The maximum takeoff weight (MTOW) of the largest Airbus aircraft at the time of writing (the A380-800) is 575 ton, which is 28% higher than that of

https://doi.org/10.1017/9781108354868.002 Published online by Cambridge University Press

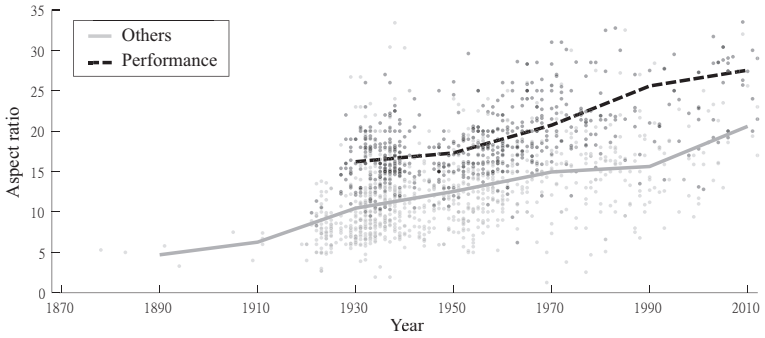

Figure 1.2 Aspect ratio by year in gliders. Each dot represents a glider design that was successfully flown.

the largest Boeing aircraft (the B747-8). Therefore, even though the A380-800 has a much longer wingspan (79.6 m for 68.4 m for the B747-8), the need for a very large area to sustain flight and the hard constraint on wingspan coming from runway width more than counteract that effect and result in a relatively low aspect ratio design. An alternative solution has been sought in the Boeing 777-9 (shown in Figure 1.3), which achieves the largest aspect ratio of any airliner to date by folding the wingtips when on the ground. By doing so, the aircraft can park in the same gates as the original B777 aircraft. Most striking still is a direct comparison between the older and newer aircraft in that chart. The wingspan of the Boeing 787 is roughly the same as that of the first-generation B747 from the 1970s, yet its MTOW is approximately a third smaller than that of the B747-100. The result is that the wings of the B787 have a much smaller area than the original Jumbo Jet for the same wingspan, and that gives the aircraft a huge boost in aerodynamic efficiency.

A similar trend can be observed in Figure 1.2, which includes almost all the gliders that have been built since the dawn of aviation.[1] A subset of gliders, designed to achieve maximum performance (one such typical vehicle is shown in Figure 1.3), is also identified in the figure. Moreover, the average aspect ratio of all vehicles flown in each decade is also included to show the underlying trend. Contrary to commercial vehicles, glider construction has little restrictions from the airport constraints, and it is of course unaffected by advances in engine technology. Therefore, gliders push the limits for aerodynamic-driven design. Comparing Figures 1.1 and 1.2 gives us a glimpse of how air vehicle configurations have evolved under different design trade-offs.

The wing aspect ratio of tube-and-wing configurations has historically been a conceptual design choice. It has been driven by the state of the art on wing manufacturing technology, and therefore follows the slow but steady increase that can be observed in Figures 1.1 and 1.2. However, the current demand for emission-free flight travel and the subsequent development of new propulsion systems, possibly based on hydrogen or electrochemical storage, may upend this trajectory. The integration of new

[1] The raw data in the graph have been retrieved from www.j2mcl-planeurs.net.

https://doi.org/10.1017/9781108354868.002 Published online by Cambridge University Press

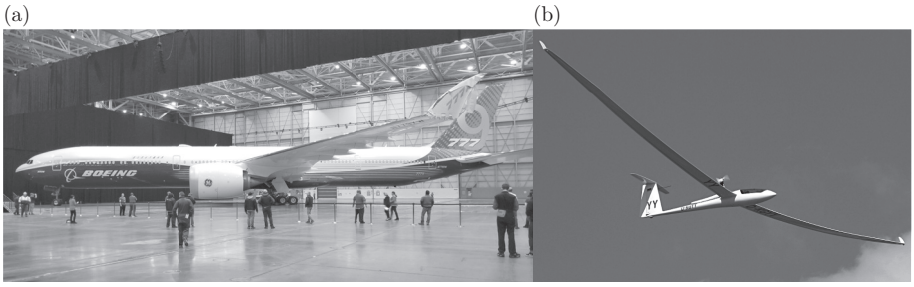

Figure 1.3 (a) Rollout of the Boeing 777-9, with folded wingtips (photo by Dan Neville). (b) A high-performance glider with the aspect ratio of 25 (photo by Juergen Lehle (albspotter.eu)).

propulsion systems brings a huge challenge to an aircraft design office, as even lighter airframes with much higher aerodynamic efficiency are needed for the viability of most new designs. A basic question arises here: How can we still ensure safe flight operation of a design built under such constraints? A large part of the answer lies in a deeper integration of the underlying disciplines, to enable the necessary trade-offs by opening the design space. More flexible aircraft break the boundary between flight dynamics and the low-frequency vibrations of the aircraft; they break the constraints to small displacements used in aerodynamic predictions, and put additional strain on the flight control systems, which need to deal with both airframe flexibility and vehicle dynamics. Navigating that larger design space is a major engineering challenge, but also a huge opportunity, the objective of this book is to give aerospace engineers the basic tools for that task.

1.2 Rigid Aircraft, Flexible Aircraft

The design offices for major aircraft manufacturers sprawl over multiple buildings in multiple sites, sometimes in multiple countries. Specialist teams have honed their skills through the cumulative effort of generations of bright engineers. The result is a very intricate but well-oiled machine with established process to ensure the safe operation of new aircraft. It is also a working environment that tends to reinforce the traditional separation between disciplines.

While there is only one end product, different representations of the aircraft are used within each discipline. On one end, we have the flight dynamics perspective. Flight dynamicists are concerned with the in-flight performance of the aircraft, and the design of the flight control systems. The aircraft is then often represented as a rigid body moving in the atmosphere and its aerodynamics given in the form of look-up tables. On the other extreme, we encounter the stress analysts, which model minute details of the airframe to understand and prevent any potential structural failure. The aircraft is now a large elastic object, typically considered in static equilibrium and under fixed forces. There are many shades of gray between both extremes and it is therefore convenient first to define the traditional scope of those key disciplines, which

https://doi.org/10.1017/9781108354868.002 Published online by Cambridge University Press

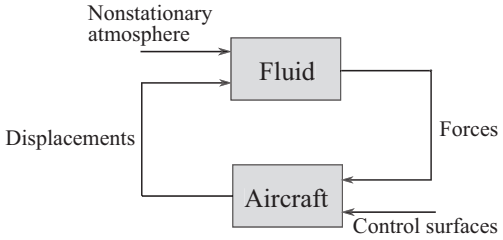

Figure 1.4 Feedback interactions between an aircraft and its surrounding fluid.

will be the starting point for the exploration in this book. Knowing where the current boundaries are will enable us to build bridges.

As we have just mentioned, *flight dynamics* is concerned with the time evolution of an aircraft in atmospheric flight, that is, establishing its trajectory and attitude under aerodynamic forces, as well as modifying those forces to steer the vehicle. It assesses the ability of the vehicle to meet its intended mission (performance) and the level of effort needed from the pilot to maneuver the vehicle (handling qualities), while providing rules for acceptable weight distribution (static stability) and configuration layout (to ensure dynamic stability). The basic interaction between the aircraft and the surrounding fluid is represented in Figure 1.4. In flight dynamics, the aircraft is typically modeled as a rigid body and the description of its interactions with the fluid is assumed to occur only through its six degrees of freedom. Moreover, in most flight regimes, the atmosphere can be considered stationary and the force resultants on the aircraft (lift, drag, moments) are uniquely determined from the instantaneous relative position and orientation (and the corresponding velocities and accelerations) of the aircraft. As a result, the fluid forces can be easily tabulated as a function of relatively few coefficients and be retrieved for flight simulation and analysis.

The evaluation of those fluid forces on the aircraft in flight is the remit of *aerodynamics*. The key objective of an aerodynamicist is to ensure that flight can be sustained across a number of design conditions at a minimum cost (drag), and also that those forces can be easily modified during maneuvers. Yet aerodynamics produces not only the force resultants that enable its flight dynamics but also the distributed loading that deforms its structure. If those deformations are sufficiently large to generate noticeable changes on the external structure, then a second feedback loop appears between structural deformations and aerodynamic forces that is studied by *aeroelasticity*. It can equally be described by Figure 1.4, although now the aircraft is also changing its geometry. We further distinguish between static and dynamic aeroelasticity, depending on whether the vehicle is in static equilibrium or not.

Regarding *static aeroelasticity*, the main interest is on the deformations that appear on the wing as it produces lift, and their effect both on (1) the final lift and drag on the wing and (2) the internal stress appearing on its airframe. Note that drag forces are affected by the shape changes due to the deformation, but they rarely deform the wing on their own. In other words, drag comes from a one-way interaction, which facilitates its study. (A corollary of this is that drag prediction is rarely within the remit

https://doi.org/10.1017/9781108354868.002 Published online by Cambridge University Press

of aeroelastic analyses.) Regarding the stresses on the airframe, they are investigated by the computation of *load cases* that size the structure. In particular, a number of steady maneuvers need to be considered for which the static aeroelastic equilibrium is sought under suitable control surface deflections and from which the distribution of applied forces (the loads) on the airframe is investigated. The worst-case conditions on each structural element define its *limit loads*, which needs to be supported without "detrimental permanent deformation" (FAA, 2011). The airframe also needs to support the *ultimate loads*, defined as the limit loads times a safety factor, without structural failure (Niu, 1999, Ch. 3). For commercial aviation, the typical safety factor is 1.5, that is, the aircraft is designed to support loads (the *ultimate loads*) that are 50% higher than the highest loads that are predicted to appear in service (its limit loads).

Often the aircraft is subjected to nonstationary atmospheric conditions, which may have a significant impact on its aerodynamic forces. When the timescales of those interactions are very large, the change of forces may mainly affect the flight dynamics, but most commonly it will also deform the airframe. In that case, we are within the remit of *dynamic aeroelasticity*. The feedback process in Figure 1.4 now needs to consider both elastic and inertial effects on the aircraft response, as well as steady and unsteady effects on the fluid. The systematic study of the response to nonstationary atmospheric conditions results in *gust loads* on the structural elements, which may also become the limit loads on certain component. Finally, as in flight dynamics, one needs to assess the dynamic aeroelasticity stability of the system, known as *flutter*.

1.3 Brief Historical Overview

Since the early days of heavier than air flights, the challenges of flexible aircraft were clearly present. Then, there was only a rudimentary understanding of aero-structural interaction and stability and controls, and most of it was empirical in nature. Here we would like to review some of the key developments along more than a century that led us to the dynamics of flexible aircraft as discussed in this book. There are several review papers and some books covering the area of aeroelasticity and/or stability and control of aircraft. Among those, we recommend the reader to explore Garrick and Reed (1981) (this one in particular provides a great list of references), Collar (1978), Perkins (1970), Abzug and Larrabee (2002), and von Kármán (1954) that served the basis for our attempt to merge these two major development paths so to better understand how we ended up where we are.

1.3.1 The Early Years

In the early 1900s, Samuel P. Langley, then secretary of the Smithsonian Institute and one of the most preeminent scientists in the United States, had been invested in the development of an airplane. The *Aerodrome* was conceived to be flown from a platform on top of a houseboat on the Potomac River. After successful subscale and unmanned flights, the second attempt to fly the manned Aerodrome on December 8,

https://doi.org/10.1017/9781108354868.002 Published online by Cambridge University Press

1903, that is, nine days prior to the famous *Wright Flyer* flight at Kitty Hawk, suffered a structural failure. As the craft accelerated during launch at an untrimmed setting, the aerodynamic loads on the front wing deformed it beyond its strength limits and resulted in its collapse. This is the first example of the importance of aero-structural considerations in trimmed flight, something that is done today for any performance assessment. It is worth noticing that in a lecture delivered to the Western Society of Engineers in Chicago in 1901 (Wright, 2001, p. 99), Wilbur Wright delineated three main issues related to fly:

> The difficulties which obstruct the pathway to success in flying machine construction are of three general classes: (1) Those which relate to the construction of the sustaining wings. (2) Those which relate to the generation and application of the power required to drive the machine through the air. (3) Those related to the balancing and steering of the machine after it is actually in flight.

He believed that the first two had been solved, and the third one was key. Indeed, the difficulties in maneuvering an aircraft were already identified during Otto Lilienthal's glider experiments several years earlier. Lilienthal's glider was made stable by positioning the center of gravity forward and controlled by moving it through body motion. The control authority for such arrangement was limited. The Wright Brothers had a very different solution to the problem: focus on the controllability and not its stability. Maybe due to their extensive bicycle experience, where the person is responsible to provide stability to the vehicle, the same idea was applied to their Wright Flyer. Particularly challenging was the lateral control, something they achieved by allowing differential elastic twist of the wings (known as *wing warping*) to change the spanwise lift distribution. This was realized by making the wing stiff in bending but soft in torsion. By taking advantage of the twist flexibility of the wing in a controlled manner, something that the Aerodrome did not have a chance to show, they were able to maneuver their aircraft. The stability was provided by the pilot employing constant corrections through the various control inputs. This highlights the two main approaches to stability: inherent stability requirement vs. stability created by the pilot (or autopilot). The wing warping concept was later employed in some successful European aircraft of the time, and this concept was also at the center of patent fights promoted by the Wright Brothers in the early years of aviation.

One of the first European concepts to employ wing warping was the Bleriot XI, shown in Figure 1.5, which was the first airplane to successfully cross the English Channel in 1909. The monoplane configuration employed wing warping for roll control and initially cruised at approximately 40 mph. The success of the Channel crossing propelled the Bleriot XI as a popular airplane, and re-engine efforts were undertaken to increase its speed. As the flight speed increased to approximately 80 mph, the wing collapsed. It was thought that it was the strength of the construction that needed improvement. So they reinforced the guy wires that supported the wings in an attempt to eliminate the problem. Unfortunately, it did not solve it and questioned the feasibility of monoplanes. In fact, the issue was found to be so critical that the British government banned monoplanes in 1912, which lasted until the approach of the Great

https://doi.org/10.1017/9781108354868.002 Published online by Cambridge University Press

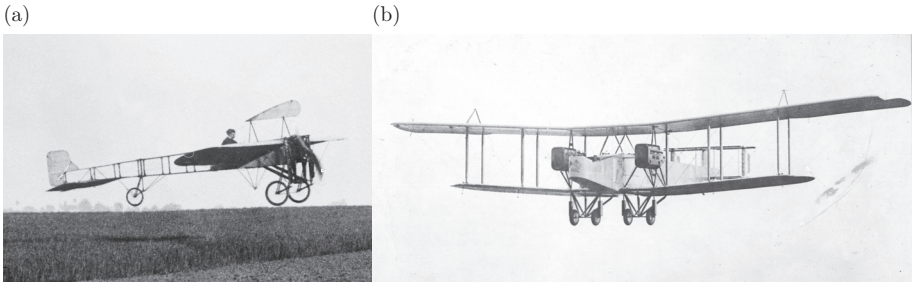

Figure 1.5 (a) Bleriot XI (photo from the Library of Congress catalogue). (b) Handley-Page Type 0 (photo from the National Archives and Records Administration).

War. This is one of the earliest records of wing divergence, a static aeroelastic instability, and, therefore, an issue of *stiffness and not strength*. A remarkable event also related to static aeroelastic instability happened closer to the end of the Great War. By 1918, the D-VIII Fokker monoplane had been designed for aerial superiority. The prototype plane flew very well with the wing structure made of two spars: the front one with a larger cross section when compared with the rear one. The concept was moved to production, but with a small requirement modification by the German Army. In order to strengthen the wing, the rear spar was to be of the same, larger cross section, as the stronger front spar. The brand new high-performance planes were given to the top pilots, who started facing wing collapse during flight. Inadvertently, by strengthening the rear-wing spar, its elastic axis was also moved aft and reduced its divergence dynamic pressure. It was not until later that this phenomenon was completely understood. Reissner (1926) presented a detailed analysis of wing torsional divergence, describing the importance of the relative position of the aerodynamic center[2] and the wing elastic axis.

Still at the time of the Great War (1914–1918), aeroelastic dynamic issues started appearing as well. A classic example is the fuselage-tail instability of the Handley Page 0/400 bomber in the 1914–17 timeframe, shown in Figure 1.5. At a certain critical speed, large couple oscillations appeared between the aft fuselage in torsion and the antisymmetric elevator motion of the biplane tail. At the time, the right and left elevators were independent from each other and connected to cables that were actuated in a way to deflect them symmetrically. Lanchester (1916) evaluated the situation conceptually and in a short technical report to the Advisory Committee for Aeronautics stated that, "[w]ithout making calculations," he concluded that "it is clear to my mind that if the elevator flaps were fixed ... an oscillation such as that described should be damped with great rapidity; in other words, to maintain such an oscillation would require some enormous direct application of energy...." And he went on to conclude that "... when the oscillation is taking place the damping action above mentioned must be absent, and one is led to look for the cause of the oscillation in some reversal of this

[2] Joukowski's theory had already showed that the pitching moment about the point one-quarter chord behind the leading edge of monoplane wings would not change with changes in the angle of attack.

https://doi.org/10.1017/9781108354868.002 Published online by Cambridge University Press

damping effect." The flexibility of the cables that made the control system allowed for asymmetric deflections of the elevators, creating rolling moment at the tail end of the fuselage. This seems to be the first formally identified flutter phenomenon in aircraft. A similar issue was encountered a year later in the DH-9 aircraft. Lanchester recommended that a single stiff torque tube should be introduced to connect the upper right and upper left elevators,[3] along with few reinforcements with the lower part of the tail. Moreover, Lanchester also recommended "for the dynamics of the tail to be studied at the National Physical Laboratory, and the matter more fully investigated there." This was undertaken by Bairstow and Fage (1916) and they confirmed Lanchester's view.

The mathematical developments related to flight lagged the initial flight experiments, that is, the experimentalists were building, testing, and flying airplanes before the mathematical models were available to help understand the various pieces of the puzzle. In 1904, British mathematicians G. H. Bryan and W. E. Williams (Bryan and Williams, 1904) were the first to apply the mathematical theory of dynamic stability previously formulated by their compatriot, Edward J. Routh (Routh, 1877). The problem of longitudinal stability and the identification of the "phugoid"[4] mode was published by Lanchester (1908). While it is acknowledged that Lanchester arrived to this conclusion on his own, Nikolai Joukowski had already identified this motion back in 1891 (Joukowski, 1891). Lanchester made observations about trajectories of a glider when "launched at the exact or natural speed, it would glide steady as if on rails." He was able to identify oscillations and their damping when perturbed from those conditions, bringing into the argument the interchange of potential and kinetic energies that determine the transient dynamics. The first complete airplane dynamics model in a rigorous mathematical way was presented by Bryan (1911), who also introduced the concept of *stability derivatives*, which separated the airplane motion into two parts, "symmetrical" and "rotative" components (now known as longitudinal and lateral, respectively, see Chapter 4), and uncovered its natural frequencies. There was no consideration of aircraft flexibility on those formulations, something that would not show up for another five decades or so. His equations of motion for a rigid body with six degrees of freedom were brought into a dimensional form in Bairstow et al. (1913), and these are still the familiar equations we use today and will see them in this book. Bairstow and his colleagues at the National Physics Laboratory also separated the equations into two independent solutions, leading to today's longitudinal and lateral ones along with the basic natural modes and frequencies. Further "wind channel" tests were conducted by them using a model scale of the Bleriot monoplane to try to correlate the stability characteristics being analyzed mathematically with the experimental observations in an effort to understand how the early airplanes were able to fly with such poor stability characteristics. Perkins (1970) presented a very nice discussion on the various consequences of those studies in the understanding of airplane stability

[3] This has become a common practice, and it can still be found in general aviation aircraft today.

[4] von Kármán (1954) argued that Lanchester may have misinterpreted the Greek word "phygoid" that "means 'to fly' in the sense of fleeing before a menace and not flying as a bird." But that has since being widely accepted to represent this longitudinal flight dynamic mode.

https://doi.org/10.1017/9781108354868.002 Published online by Cambridge University Press

and controls. As he stated there, "the perplexing fact, ... when airplanes encountered the instability directly forecast by the mathematicians, the airplanes go along quite well and flew anyway." It was not until the mid of the twentieth century when stability and controls, and the role of the human pilot in the loop, were brought together in the studies at the National Advisory Committee for Aeronautics (N.A.C.A.) "at Langley and Ames laboratories [in the U.S.A.] and by researchers of the Royal Aircraft Establishment (RAE) in Great Britain."

It was during the 1920s that a series of flutter problems came to plague aviation, mainly due to wing-aileron flutter, which was first identified in 1922. This new dynamic instability involved the inertial forces on the wing deflecting the aileron in a particular phase in order to increase the motion in the direction of the initial motion. As was in the case of the Handley Page 0/400, the flexibility of the cables allows aileron deformation around the setting point when subject to inertial accelerations. von Baumhauer and Koning (1922) pointed out the importance of the inertia coupling for the flutter onset and proposed to solve it by *mass balancing*: by bringing the center of mass of the control surface to be at its hinge location or forward of it. During this decade, significant aerodynamic developments were achieved. Since the characteristic timescales of the structural motions may be comparable to the convective timescales in the flow, these led to the need of theories of nonstationary flows around moving airfoils. Studies were initially developed by Ludwig Prandtl and his students in Göttingen. The first person to successfully complete his dissertation on airfoil theory was W. Birnbaum, who published the classical vortex theory of two-dimensional (2-D) steady flow of thin airfoils (Birnbaum, 1923),[5] followed by the harmonically oscillating airfoil in uniform motion (Birnbaum, 1924). In his work, he expressed the wake vorticity as the function of the airfoil-bound vorticity in order to obtain an integral equation relating pressure over the airfoil with its normal velocity–a key step employed by Theodorsen over 10 years later for harmonically oscillating airfoils (Theodorsen, 1935). Furthermore, the concept of *reduced frequency* was already employed in his work. The approach, however, did not quite work for reduced frequencies (as defined in Section 3.3.3) greater than 0.2. Also from Prandtl's group, Wagner (1925) presented an alternative solution to the problem of harmonic nonstationary flow by introducing the solution to a step change in the angle of attack, which is known today as the indicial solution. The resulting function satisfying Kutta-Joukowski[6] trailing-edge condition and giving the growth of lift with distance traveled is known as the Wagner's function (see Section 3.4.3). Glauert (1929), following Wagner's methods, addressed flat plate airfoils undergoing steady pitch oscillations. Glauert was then able to numerically solve the problem without the convergence difficulties experienced by Birnbaum. In that same year, Hans-Georg Küssner (1929) presented a seminal paper on flutter prediction utilizing improvements on Birnbaum's method. He showed improved numerical convergence to reduced frequency of order

[5] Max Munk (1922) had published his thin airfoil theory shortly before Birnbaum, while H. Glauert (1923) provided an alternative formulation the year after.

[6] We follow here von Kármán (1954, Ch. 2), even though many references simply refer to it as the Kutta condition.

https://doi.org/10.1017/9781108354868.002 Published online by Cambridge University Press

1 in beam-type problems with bending and torsion and including aileron. At the end of this decade, known as the "flutter decade," Frazer and Duncan (1928) summarized their studies in flutter of wings that, according to Collar (1959), became known to aeroelasticians as the "Flutter Bible."

The advent of stressed skin construction finally brought about the end of the biplane dominance and the dominance of the monoplane around 1930s. By then, the flying speeds were such that the flexibility could not be ignored anymore. Flutter assessment in every design became a necessity. That was also the decade of intensive theoretical developments. Duncan and Collar (1932) extended the theory of Glauert to include wing translation and rotations. Theodorsen (1935) at the National Advisory Committee for Aeronautics (N.A.C.A.) Langley Research Center worked on the flutter problem and presented the theory of the 2-D oscillating thin airfoil in potential flow undergoing simple harmonic motion in pitch and plunge, and aileron-type motions. He separated the noncirculatory terms from the circulatory ones and, like Birnbaum, by imposing the Kutta-Joukowski condition at the trailing edge he connected the wave vorticity with the bound vorticity through an integral relation. The solution led to a combination of Bessel functions that is now known as the *Theodorsen function* (see Section 3.3.3). These extended quasi-steady constants used before have now become frequency dependent. This exact solution (in contrast to the numerical approximations made by Glauert and Küssner that limited the reduced frequency applicability of their approaches) for the simple harmonic motion of thin flat airfoil in potential flow has become the cornerstone for the *strip theory* widely used in industry for simple flutter estimation, particularly for high-aspect-ratio wings. While there are some clear similarities between Theodorsen's approach and the earlier ones, particularly Birnbaum's, Wagner's, and Glauert's, here there is no use of the Routh's discriminants as widely used before since the flutter determinant is complex and both real and imaginary parts must be satisfied simultaneously. This led to approximate ways of determining the flutter solution, including the so-called *k*-method introduced by Smilg and Wasserman (1942). It is worth mentioning that about the same time, Cicala (1935) in Italy independently developed the oscillating flat plate solution. Theodorsen and Garrick (1938) conducted numerous trend studies for the various parameters of a typical section: center of mass, elastic axis, mass ratio, bending/torsion frequency ratio, etc. At some point, it became apparent from experiments that flutter usually involved more degrees of freedom than the usual two or three used in the typical section calculations. Duncan (1939) suggested then to use normal modes to represent the complete participation of the aircraft elasticity into the problem and that would save on computation. Indeed, normal modes have been used up to this day for describing the response of the linear deformed aircraft.

An initial theoretical study of aircraft encountering discrete gust was published in the first N.A.C.A. report to the U.S. Congress (Wilson, 1916). It contains the aircraft equations of motion with its stability derivatives and a very simple model of the aircraft response to discrete gust encounter without unsteady aerodynamic effects. The analytical solution for the interaction of a gust with an airfoil was derived by Bill Sears in his doctoral research under von Kármán's supervision at Caltech's Guggenheim Aeronautical Laboratory (GALCIT) (Sears and von Kármán, 1938). In his memoirs, Sears

https://doi.org/10.1017/9781108354868.002 Published online by Cambridge University Press

(1994) recounts how von Kármán proposed unsteady aerodynamics as a research topic to him after a visit to Göttingen in 1936. Küssner (1936) had showed to him his solution to the "sharp-edge" gust problem that seemed to have shown that the problem of a body moving on a fluid and its reciprocal (the fluid moving with respect to the body) had different solutions. Very soon after this, Sears identified a sign error in Küssner theory! In other words, the career of one prominent aerodynamicist (and one of the key solutions in this book) is the result of an algorithmic mistake by another now-famous aerodynamicist. The frequency-domain solutions derived during this time have been a cornerstone of dynamic aeroelastic studies ever since.

It was also during the 1930s and 1940s that elastic distortions began to affect rigid-body stability and control of the aircraft. One of the first documented work discussing stability with aeroelasticity was presented by Pugsley (1933), who was part of the Royal Aircraft Establishment (RAE). He investigated the impact of the elastic changes in wing twist and its consequence in the longitudinal stability of the aircraft. Following this, Bryant and Pugsley (1936) investigated the impact of the antisymmetric wing deformation on the lateral stability of the aircraft. The elastic distortion on the longitudinal stability has proven to be much more serious (Collar, 1946), and that included the effects of tail and fuselage distortion. At the time, design criteria had been developed for wing stiffness, but not for other parts of the aircraft, including the tail. From a coupling with controls, Cox and Pugsley (1932) and Duncan and McMillan (1932) investigated the then newly discovered aeroelastic-induced control problem: *aileron reversal*. In this phenomenon, with the increase in dynamic pressure, the change in lift generated by the deflection of the trailing-edge control surface is counteracted by an opposite twisting of the wing. While at the beginning this presents itself as a reduction in control effectiveness, at a particular value of the dynamic pressure, one effect can cancel the other, and there is no rolling moment resulting from the aileron deflection; this dynamic pressure is known as the aileron reversal dynamic pressure. Although not a stability issue per se, this was the first important coupled aeroelastic–flight mechanics problem which became a critical design consideration for World War II (WWII) fighters.

During the war period, the trend to higher speeds and all-metal aircraft persisted. Many flutter problems occurred during this time, particularly related to stores being carried under the wing (e.g., a tip-tank flutter problem occurred with the P-80 aircraft) and various battle damages and field fixes that altered the mass and stiffness of the airframe. Another issue that started concerning the engineers of the time was the compressibility effects in aileron reversal, further augmented by the tapered wings. At this point in time, the structural dynamics of the aircraft was still in its infancy and mostly unconnected with the overall aeroelastic analysis of the aircraft. In fact, the airplanes of the World War II that took flutter into consideration in their design had the analyses done for the wing and/or tail (separately) assuming a representative section. That section, converted into a "typical section" had no more than three degrees of freedom: plunge (for bending), pitch (for twisting), and control surface (for the elastic deformation of aileron or elevators). The idea of bringing the rigid-body degrees of freedom to the mix still seemed unnecessary. A very nice account of the efforts at the

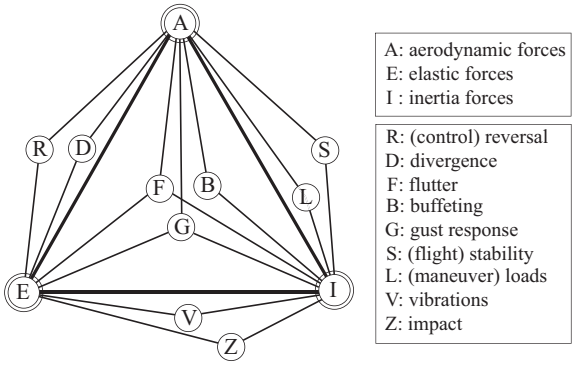

Figure 1.6 *Collar's triangle* of aeroelastic interactions.

time can be found in a review paper by Collar (1946). There he proposed a triangular graphical representation of the various disciplines that constituted *aeroelasticity*[7] and became known as the *Collar's triangle*, as shown in Figure 1.6. The figure describes the three main forces that make the field of aeroelasticity: elastic, aerodynamic, and inertial forces, and from there, various problems were derived, either inside or outside the triangle. Most of them are discussed in later chapters in this book. In a later account (Collar, 1978), Garrick, a research scientist and manager first at N.A.C.A. and later at National Aeronautics and Space Administration (NASA), and a coworker of Theodorsen, qualified this graphical representation as "it is both a chart and a compass for aeroelasticians." It seems Collar was the first to formally present the idea of combining elasticity and stability/controls together, thus resulting in the *dynamics of deformable aeroplanes*. According to Collar:

> ... dynamics of a deformable aeroplane – suggests the formal solution at once. We select as generalised co-ordinates quantities defining the translational and angular freedoms of the aeroplane as a rigid body; we add co-ordinates representing the control surface angles, tab angles, stick and pedal movements, and with these we include co-ordinates to represent the freedoms due to automatic controls; finally we introduce a number of co-ordinated sufficient to describe the modes–normal or otherwise–of elastic deformation of the aircraft. We then derive, in terms of the inertia and elastic properties of the aircraft and the forces, the complete Lagrangian equations of motion ... (1946, p. 630).

While visionary, Collar also faced the limitations at the time: "... we obtain a set of simultaneous differential equations, probably in twenty to thirty degrees of freedom, ... From the practical viewpoint, of course the labour of dealing with such a set of equations is prohibited at present." Just for reference, today we deal with thousands of equations routinely, empowered by modern computers and numerical methods.

[7] According to Collar (1978), the term *aeroelasticity* was coined by Roxbee Cox and Alfred Pugsley in the early 1930s, and it may have been inspired by the term *photoelasticity* in vogue among experimentalists at the time.

https://doi.org/10.1017/9781108354868.002 Published online by Cambridge University Press

1.3.2 The Jet Age

Up to the mid-1950s the aeroelastic and flight dynamics developments continued their courses separately, except for the control effectiveness and stability considerations that bridged the two. As von Kármán highlighted in his book (von Kármán, 1954), "The science of aeroelasticity, including flutter theory, is now in a period of active development." Small corrections to the effect of flexibility on the airplane stability were made assuming small aeroelastic contributions to the rigid airplane stability derivatives obtained from wind-tunnel testings. However, the increase in aircraft size and flying speed led to combined studies. One of such studies is presented in the report by the J. B. Rea Company (Rea, 1957), where a comprehensive study was conducted to bridge the aeroelasticity developments with the flight dynamics of the time. More like a handbook, this report was created by several authors, including Y. C. Fung from Caltech, for the practicing engineer to "give methods for incorporating aeroelastic effects in equations of motion as well as techniques for obtaining the solutions," mostly through matrix methods. As also emphasized there, "many of the techniques of analysis are still in a state of development."

The early airplanes were far from rigid, but their low speeds masked the elastic effects, particularly in view of all the other challenges they were facing then. With the increase in flying speed along the years, two relevant effects came to play: the relative increased flexibility effects in the structure and the compressibility effects in the aerodynamics. The relative flexibility of a structure is directly related to the dynamic pressure and is dependent on the air density and the square of the airspeed. The compressibility effects come in the form of change in aerodynamic coefficients, center of pressure, and aerodynamic center, ultimately impacting the stability of the aircraft. Aircraft aeroelastic problems were markedly accentuated with the higher speeds provided by jet propulsion. And with those higher speeds, the wings were swept, bringing additional challenges as well. The airplane that brought the aeroelastic problem to everyone's attention during that phase was the Boeing XB-47 bomber, as shown in Figure 1.7. It was known that the airplane would have flexible wings, but at the end,

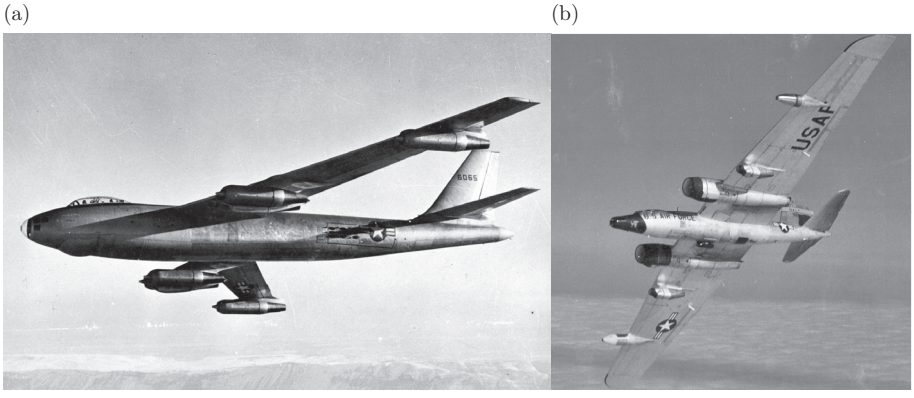

Figure 1.7 (a) Boeing XB-47. (b) Martin RB-57F Canberra (photos from the U. S. Air Force).

https://doi.org/10.1017/9781108354868.002 Published online by Cambridge University Press

for a 116-foot span wing, it showed deflections of 35 ft. between the maximum positive and negative loads (Perkins, 1970), representing a tip-deflection amplitude of the order of 30% of its semispan! Along with that, came additional challenges with stability and control. For example, during pull-up maneuvers, the wings would deflect up, inducing an effective down twist, which in turn would alter the wing aerodynamic center. This would have a direct impact on the tail downwash and its effectiveness. The elastic wing deflection would also move the center of gravity by 15% forward during a pull-up maneuver, altering the aircraft stability (Cook, 1991).

A major milestone in bridging aeroelasticity and flight dynamics came with the work of R. D. Milne (1962). In his work, Milne took the equations of motion of Bairstow et al. (1913) and augmented them with the structural equations in the form of beam or plate theories solved with the Rayleigh–Ritz method, or the use of equivalent influence functions for more general structures. He also introduced the powerful concept of *mean axes*, which will be further discussed in Chapter 6. During this time, a new aeroelastic instability was found: *body-freedom flutter*. This is a flutter mechanism that involves the participation of at least one rigid-body motion (typically pitch) of the aircraft along with elastic modes. This coupling between the rigid-body motion and elastic motion is facilitated either by a reduction in pitch inertia of flying-wing configurations, where the resulting increase in the short-period frequency gets closer to the first bending mode of the wings, or by increasing the wing flexibility and bringing its frequency down and in the vicinity of the short-period mode. While this was already faced by the Horten high-aspect-ratio flying-wing sailplane in the pre-WWII Germany, it was not until the General Dynamics RB-57F that the problem came screaming to the aeroelasticians. This aircraft, as shown in Figure 1.7, was a new high-altitude reconnaissance aircraft based on a conversion of the existing Martin B-57 but with larger wings, bringing its first bending frequency to 1.5 Hz (Love et al., 2005). The instability was discovered during flight tests and just beyond the limit speed of the aircraft – with two more additional flutter incidents as a result of unintentional overspeed. In fact, a similar problem was later found in the Northrop B-2 bomber but, once again, outside its operational envelope (Jacobson et al., 1998).

By the 1960s, closer connections between aeroelastic and flight dynamics considerations were clearly needed due to: "1. The considerable increase in speed. 2. The thinner shapes required for transonic and supersonic flight. 3. The new airframe designs such as variable geometry. 4. The new generation of commercial aircraft: stretching of present long range liners, Jumbojets, Supersonic transports. 5. The growing interest in low level flight for military purposes" as identified and addressed by an Advisory Group for Aerospace Research and Development meeting in 1969 (Anonymous, 1969). This was a coordinated effort among the North Atlantic Treaty Organization nations to bring theoretical and experimental aeroelastic methods into flight mechanics. An example is the work of Dusto (1969) from the Boeing Company, who employed Milne's mean-axes approximation along with structural influence coefficients to obtain steady and unsteady stability derivatives through residualization. This approach was applied to evaluate the stability of two aircraft of the time: B707 and the SST. Chevalier et al. (1969) found the elasticity effects on the static longitudinal

stability to be "large and unfavorable" while not greatly affecting their dynamic stability characteristics. However, the authors make the point that "results indicate that as the structural frequencies approach the frequency of motion of the airplane (ratios less than 4:1), major effects might occur."

There were finally two main developments that took place in the late 1960s that have impacted the way we evaluate the flutter today. One was the development of the doublet-lattice method (DLM) by Albano and Rodden (1969), and the other was the initial development of a common structural dynamics analysis software for NASA's various centers, named NASA STRucture ANalysis or NASTRAN. This eventually went commercial (MacNeal and McCormick, 1972), evolved along the years, and through its aeroelastic solver incorporated the DLM solution. This has become the most used aeroelastic solver in the aerospace industry.

With the development of high-bandwidth actuators and control systems theory and hardware, the possibilities of altering the dynamics and response of an aircraft through active controlled closed-loop action of its control effectors became a reality.[8] The increased importance of the active control system (ACS) and its interplay with the flexible airframe has led to an explicit inclusion of their combined effects in the analysis, design, and certification (when applicable) of new aircraft. Known as aeroservoelasticity (ASE), this area of study encompasses the alleviation of loads, both maneuver and gust, fatigue life extension, control of elastic modes and overall deformation, stability and flutter margin augmentation, and improvements in ride quality (Hönlinger et al., 1994).

Although some theoretical studies were conducted in the previous decade, one early example of experimental tests on the impact of the ACS on the airframe loads can be found in the work of Payne (1953). Although the autopilot was not designed for load alleviation, the series of flight tests with a small transport plane[9] resulted in gust loads being attenuated by approximately 7% when the autopilot was engaged. A more comprehensive gust-load alleviation (GLA) study was presented by Phillips (1957). In his report, a review of the various effects related to controlling the load is presented, including sensors and actuators. Two dedicated flight tests had just finished: one targeting improvements in ride quality while measuring the impact on the structural loads due to gust, and the other measuring the impact of a yaw damper on reducing vertical tail loads. For the former, the vane-controlled gust-alleviation system flight test was studied by Chris Kraft (Kraft, Jr., 1956), later to become the mastermind of space flight management for all future NASA space manned missions. The gust-load investigation showed mixed results: there was actually an increase in structural loads while improving passenger comfort during light turbulence, and for severe turbulence, the

[8] It is interesting to notice that the idea of active feedback control had been known for a while (e.g., Millikan, 1947). In terms of flutter control, for example, Bisplinghoff et al. (1955) indicate that "... exists an excellent possibility of improving flutter performance by ... rapidly responding automatic control system, actuated in closed-loop fashion by the motion to be stabilized. However, we cannot count on the human pilot to compensate for flutter ... because the frequencies are too high ...."

[9] The report does not specify the airplane model, but it contains drawing of it. It is our understanding that the aircraft used for these tests was a version of the Convair CV-240.

https://doi.org/10.1017/9781108354868.002 Published online by Cambridge University Press

system was expected to reduce the wing loads but increase the loads in the tail and other structural components–a well-known phenomenon understood today.

With larger aircraft being developed, the U.S. Air Force established the Load Alleviation and Mode Stabilization (LAMS) program in the second half of the 1960s to study the impact of ACS to alleviate gust loads and enhance fatigue life in more flexible aircraft. The final report from Burris and Bender (1969) describes the extent of the study involving U.S. industry and government to demonstrate the technology in a modified B-52E test vehicle. That included the addition of hydraulic powered controls and fly-by-wire pilot station, besides the instrumentation required for flight tests, specifically designed to alleviate structural loads during atmospheric turbulence encounters. The program successfully showed that the LAMS combined with the ACS provided significant reduction in the fatigue damage rate while satisfying the design and performance criteria established at the time. A parallel analysis-only study was also conducted in the C-5A Galaxy to show that the technology could be used in other large aircraft.

There were significant ASE activities in the 1970s, and some key examples are presented in the review report of Regan and Jutte (2012) as well as in the comprehensive review of Livne (2018). The B-52 LAMS studies continued with the B-52 Control Configuration Vehicle (CCV) program, a pioneering effort on active aeroservoelastic control. The testing aircraft was modified to include canards and ventral vanes, and external stores were mass balanced to bring flutter into the operational envelope of the aircraft. In this way, flight tests for active flutter control could be safely conducted since in the case of instability, the stores could be quickly ejected from the aircraft, restoring its initial stable characteristics. The CCV program was able to successfully show simultaneous improvements in flutter mode control, maneuver load alleviation (MLA), ride control, fatigue reduction, and stability augmentation (Roger and Hodges, 1975). Another early example of an aircraft incorporating active control is the Lockheed C-5A, also a direct extension of the initial analytical studies as part of the LAMS program (Burris and Bender, 1969). The aircraft was suffering from fatigue life problems related to wing bending loads. The Active Lift Distribution Control System (ALDCS) was developed to reduce wing stress during turbulence encounters and maneuvers (Disney, 1975). By sensing forward and aft vertical wingtip accelerations along with inertial reference system signals, the ALDCS actuated ailerons and inboard elevators to reduce the wing root bending moment by more than 30%, although it also observed increases in torsional loads. The system was eventually superseded by a structural modification that added 5.5% of the initial empty weight of the aircraft. An interesting example of increasing wing span (5.8%) to reduce total drag (3%) and avoid a mass increase (1.25% of gross weight) is found in the Lockheed L-1011-500. The ACS was put in place to provide maneuver load alleviation (MLA) and gust load alleviation (GLA) by using the horizontal stabilizers and ailerons without significant structural modifications. Another example of GLA is found in the Northrop B-2 Spirit aircraft, where gust loads were sizing the vehicle (Britt et al., 2000). The GLA system employs the inboard elevons and a dedicated GLA surface at the aircraft centerline. Due to undesirable excitation of the aircraft's first symmetric bending

https://doi.org/10.1017/9781108354868.002 Published online by Cambridge University Press

mode, the outer elevons are used out of phase to damp the vibration. In terms of controlling the ride quality, an early example is the structural mode control system present in the Boeing's B-1 Lancer aircraft. By using dedicated active canard-control surfaces and colocated accelerometers, the system suppressed vibrations at the pilot station, particularly during gust encounters. Parallel studies were also being carried out in Europe. In particular, the German Aerospace Center (DLR, formerly known as DFVLR) conducted flight tests targeting ride quality and the control of flight dynamics characteristics, particularly the short-period mode, as exemplified by the Open Loop Gust Alleviation in the late 1970s and early 1980s, followed by the Load Alleviation and Ride Smoothing system in the 1980s and early 1990s. In this latter program, full fly-by-wire capability was deployed with additional direct-lift-control flaps in DLR's twin-jet test aircraft, which showed reduction in the longitudinal and vertical accelerations with a combination of lift and drag control devices but marginal reductions in the wing root bending moment (Hahn and König, 1992). Many other examples can be found from a more fundamental research on exploring ACS for aeroelastic and flight dynamics improvements. One example is the successful series of wind-tunnel studies of two SensorCraft concepts (Lucia, 2005) for load alleviation and stability enhancements. The blended wing body concept (Vartio et al., 2005) and the joined-wing configuration (Scott et al., 2011) were tested both with a rigid support and with attachment to a pitch-and-plunge apparatus in the Transonic Dynamics Tunnel at NASA Langley. The aeroelastically scaled models showed the importance of including rigid-body degrees of freedom when assessing and controlling the stability (flutter) and gust response of flying wings and more flexible concepts.

While these are examples of solutions developed to mitigate a design problem, recent commercial aircraft have been developed with these technologies in mind. An early example is the Airbus A320 (entered service in 1987) that incorporated a load alleviation function (LAF) that actuated a combination of ailerons, spoilers, and elevators while sensing the inertial load factor. The increase in actuator utilization might have led to its de-activation in its derivatives and later reintroduction in the Airbus A330 (entered service in 1994) and A340 (entered service in 1993) for MLA and improved flying qualities (Regan and Jutte, 2012). Similarly, the Boeing B787 (entered service in 2011) includes MLA and ride quality enhancements through the use of ailerons, spoilers, and flaperons. According to Norris and Wagner (2009, p. 87), several thousand pounds of weight were taken out of the design by actively reducing the maneuver loads.

1.3.3 Towards Sustainable Flight

After some niche human-powered aircraft developments primarily led by Paul MacCready in the 1970s and 1980s, where the extremely light structural constructions and flexible airframe brought challenges in the coupled aeroelastic–flight dynamics behavior, it was really the high-altitude, long-endurance (HALE) planes from the late 1980s and until now that have really challenged the then state of the art in this field.

https://doi.org/10.1017/9781108354868.002 Published online by Cambridge University Press

During the 1990s and early 2000s, a joint NASA and industry initiative established a long-duration Earth science and environmental missions at high altitudes known as Environmental Research Aircraft and Sensor Technology (ERAST) program.[10] Among the industry participants, Aerovironment (founded by MacCready) had developed Helios, an ultra-lightweight flying-wing solar-powered aircraft with a constant chord wing of 247 ft. (75.3 m) span and an aspect ratio of 30.9. The airplane had many successful flights, including an altitude record of 96,863 ft. in 2001. In 2003, equipped with a fuel cell for longer duration flight, Helios encountered a shear layer at approximately 3,000 ft. over Hawaiian waters, which excited an instability that led to the loss of the aircraft. As part of the mishap investigation, Noll et al. (2004) concluded "[that] more advanced, multidisciplinary (structures, aeroelastic, aerodynamics, atmospheric, materials, propulsion, controls, etc.) time-domain analysis methods appropriate to highly flexible, morphing vehicles [be developed]." They also stated that "[t]he Helios accident highlighted our limited understanding and limited analytical tools necessary for designing very flexible aircraft and to potentially exploit aircraft flexibility." This motivated many in the research community to look into the problem, and for the next decade, many studies were conducted coupling nonlinear aeroelasticity and flight dynamics, primarily targeted to the HALE class of aircraft. Most of the work has been numerical in nature, and few experimental studies in wind-tunnel (e.g., Tang and Dowell, 2001) and flight tests (e.g., Cesnik et al., 2012; Ryan et al., 2014) attempted to support those developments. During that time period, there were also several studies in ASE targeting control of loads (e.g., Boeing/AFRL/NASA Active Aeroelastic Wing Program) and stability (e.g., AFRL/Boeing/NASA B-52E flutter, loads and ride control program) (Friedmann, 1999; Livne, 2018; Livne and Weisshaar, 2003), and we encourage the reader to explore the rich literature available in the topic.

While climate change had been identified as a threat to life on Earth for quite some time, it was not until the early 2010s that the aviation industry committed itself to reduce emissions. NASA conducted studies in what they referred to as the N+1, N+2, and N+3 aircraft of the future. Part of these studies was the identification of various technologies that could reduce fuel burn (and consequently emissions) and noise. Among the investigated technologies, higher-aspect-ratio wings for lower induced drag was one of the key airframe concepts with the largest impact.[11]

An example of how the aspect ratio can impact fuel burn for a long-range commercial transport aircraft is included in Figure 1.8. It shows curves for optimum designs (i.e., Pareto fronts) obtained from a blend between minimizing fuel burn

[10] Early concepts of this class of aircraft, including Theseus, Pathfinder, and Helios, were in part the motivation for this book's second author to spearhead his research interests in this area. He first involved his Ph.D. advisor, Dewey Hodges, while a postdoctoral fellow at Georgia Tech (Cesnik, 2023). As he moved to the faculty at MIT and later to the University of Michigan, he extended his research activities in the field of coupled nonlinear aeroelasticity and flight dynamics. This book's first author's doctoral and postdoctoral studies at the University of Michigan were directly connected to those activities.

[11] More recent designs such as the Boeing 787 and the 777X are examples of higher aspect-ratio configurations that resulted in more flexible wings, as shown in Figure 1.1.

https://doi.org/10.1017/9781108354868.002 Published online by Cambridge University Press

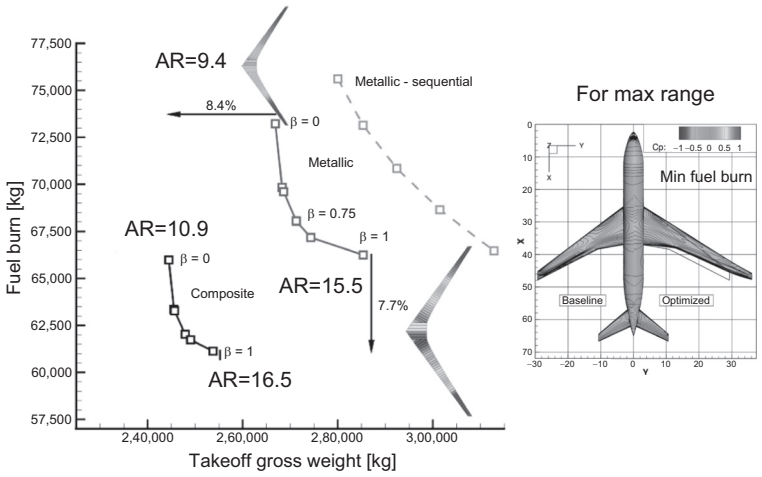

Figure 1.8 Highly efficient flight performance leads to high-aspect-ratio wings (adapted from Kennedy et al. (2014)).

and takeoff gross weight, where β is the weight between both cost functions, that is, cost metric $= \beta(\text{fuel burn}) + (1-\beta)(\text{takeoff gross weight})$ (Kennedy et al., 2014). For $\beta = 1$, that is, when all the emphasis is on minimizing fuel burn, the optimized wing aspect ratio for a simultaneous aero-structural optimization is 65% higher than the one when takeoff gross weight is minimized. While the high-fidelity MDO behind these calculations did not include dynamic stability considerations (i.e., flutter), it clearly shows the trends. Moreover, it also shows the importance of a simultaneous optimization instead of a sequential one. To achieve this higher aerodynamic efficiency while keeping the structural weight low, the resulting designs are naturally more flexible and more prone to aeroelastic effects. Moreover, the fact that the airframe elastic frequencies go down implies that they now cannot be clearly separated from the flight dynamics frequencies. Therefore, the problem has become intertwined and the coupled nonlinear aeroelastic/flight dynamics needs to be considered when sizing and certifying these new designs. These challenges have brought a new wave of research and development needs, and while these are still ongoing, we expect the new methods and capabilities to directly impact our next generation commercial transport aircraft development and support the zero-emission efforts our industry is committed to. Moreover, the coupled nature of the problem put even more demand on a holistic and integrative approach to the problem. The originally separated objectives of load alleviation, flutter enhancement, and ride and handling qualities, all need to be treated and addressed simultaneously by the appropriate manipulation of the rigid and elastic modes. The deeply coupled nature of this multidisciplinary problem creates new demands on the way the engineers are educated and the way aircraft companies must organize their engineering departments. We are seeing a renascence of aeroelasticity through the future environmentally designed "deformable aerial bodies." These are very exciting times indeed.

https://doi.org/10.1017/9781108354868.002 Published online by Cambridge University Press

1.4 Some Basic Concepts

This book is mostly concerned with aircraft dynamics, which will be described within the framework of classical mechanics. Some relevant conventions and formalisms are therefore introduced first in Section 1.4.1. Moreover, for the analysis of the vehicle performance and/or design of control systems, it is often also convenient to consider its linearized response. Here, the mathematical framework of linear time-invariant (LTI) dynamical systems is particularly useful, and some basic definitions are introduced in Section 1.4.2.

1.4.1 Dynamics

The most general description of the dynamics of a deforming aircraft is obtained within the framework of continuum mechanics; yet, in practice, we always use a finite-dimensional representation of the vehicle obtained from a spatial discretization of the physical domain. The resulting set of parameters is known as *generalized coordinates*, and the vector space in which they lie is called the *configuration space*. Let N_q be the number of generalized coordinates. We aggregate them into a column vector, $\mathbf{q} = \begin{Bmatrix} q_1 & q_2 & \dots & q_{N_q} \end{Bmatrix}^\top$, and the problem of describing the flexible aircraft dynamics becomes the evaluation of the time history $\mathbf{q}(t)$ during the events of interest. For example, in a finite-element discretization of a wing, the generalized coordinates are the time-dependent displacements at all the grid nodes, and we may be interested in tracking their values as the aircraft performs a certain maneuver. The generalized coordinates, however, do not uniquely define the instantaneous state of a moving or vibrating wing, which also depends on the instantaneous velocities at the nodes. We define then the *phase space* (or state space) as a representation of the mechanical system that uniquely determines its instantaneous state, given by a state variable $\mathbf{x}^\top = \begin{Bmatrix} \mathbf{q}^\top & \dot{\mathbf{q}}^\top \end{Bmatrix}$. Consequently, we often need to distinguish between *degrees of freedom*, $\mathbf{q}(t)$, which are the generalized coordinates that need to be solved in the equations of motion, and *states*, $\mathbf{x}(t)$, which are needed for phase-space descriptions.

Hamilton's principle provides the framework to determine the dynamics of a flexible body within a finite interval $0 \leq t \leq t_f$ for given initial conditions and external forces. It states that the trajectory of a mechanical system in the configuration space is a stationary point of the system Lagrangian, $\mathcal{L} = \mathcal{T} - \mathcal{U}$, where $\mathcal{T}$ and $\mathcal{U}$ are the kinetic and internal (or strain) energy of the system, respectively. For a flexible body, this results in enforcing that perturbations of the system Lagrangian cancel the virtual work of the external forces, $\delta\mathcal{W}$, when obtained under the same virtual displacement field, that is,

$$\int_0^{t_f} (\delta\mathcal{T} - \delta\mathcal{U} + \delta\mathcal{W})\, \mathrm{d}t = 0. \tag{1.1}$$

This expression is valid independently of the selection of reference frame or any other parameterization of the flexible body kinematics. If a phase-space description (with the generalized velocities replaced by generalized momentum using a Legendre

https://doi.org/10.1017/9781108354868.002 Published online by Cambridge University Press

transformation) is now introduced, it results in the formalism of Hamiltonian mechanics, which will be used later in this book in Section 8.6. The starting point in most of this book is, however, the framework of Lagrangian mechanics, in which the solution is sought in terms of a finite number of generalized coordinates. In that case, Hamilton's principle results in *Lagrange's equations of motion* (see Chapter 1 of Géradin and Rixen (1997) for the derivation), which are written as

$$\frac{\mathrm{d}}{\mathrm{d}t}\frac{\partial \mathcal{T}}{\partial \dot{q}_i} - \frac{\partial \mathcal{T}}{\partial q_i} + \frac{\partial \mathcal{U}}{\partial q_i} = f_{qi}, \quad \text{for } i = 1, \ldots, N_q, \tag{1.2}$$

with f_{qi} being the generalized force associated with the generalized coordinate q_i. They satisfy $\delta\mathcal{W} = \delta\mathbf{q}^\top \mathbf{f}_q$. If $\|\mathbf{q}\| = \sqrt{\mathbf{q}^\top \mathbf{q}}$ is sufficiently small, linear dynamics can be assumed. In that case, the kinetic and strain energies are written, respectively, as

$$\mathcal{T} = \frac{1}{2}\dot{\mathbf{q}}^\top \mathbf{M}\dot{\mathbf{q}} \quad \text{and} \quad \mathcal{U} = \frac{1}{2}\mathbf{q}^\top \mathbf{K}\mathbf{q}, \tag{1.3}$$

where $\mathbf{M}$ and $\mathbf{K}$ are the mass and stiffness matrices associated with the generalized coordinates. The linear dynamics of a flexible body in an inertial frame can then be approximated as

$$\mathbf{M}\ddot{\mathbf{q}} + \mathbf{K}\mathbf{q} = \mathbf{f}_q, \tag{1.4}$$

which is solved together with the initial conditions $\mathbf{q}(0) = \mathbf{q}_0$ and $\dot{\mathbf{q}}(0) = \dot{\mathbf{q}}_0$. This basic description is often augmented with a model for viscous damping, as will be done later in this book.

1.4.2 Linear Dynamical Systems

Under sufficiently small perturbations, and if there are no explicit functional dependencies with time in the underlying physical processes (e.g., mass assumed to remain constant), we can treat many problems in this book as finite-dimensional LTI systems with multiple inputs and outputs. The definition of inputs and outputs depends on the system and the particular problem of interest. For a wing described by Equation (1.4), the inputs may be deflections of a trailing-edge flap that modify the force vector $\mathbf{f}_q$, and the outputs may be the resulting elastic displacements at certain points of the wing, which can be obtained from the generalized coordinates $\mathbf{q}$. Let N_u be the number of independent inputs and N_y the number of outputs. We define the input and output vectors as $\mathbf{u}(t)$ and $\mathbf{y}(t)$, respectively, and describe their relation using block diagrams that encapsulate the internal dynamical processes, such as the basic one shown in Figure 1.9.

In this book, we consider three different, but also equivalent, representations of the input–output dynamics of an LTI system, namely by means of a state-space

Figure 1.9 Input and output on a dynamical system.

https://doi.org/10.1017/9781108354868.002 Published online by Cambridge University Press

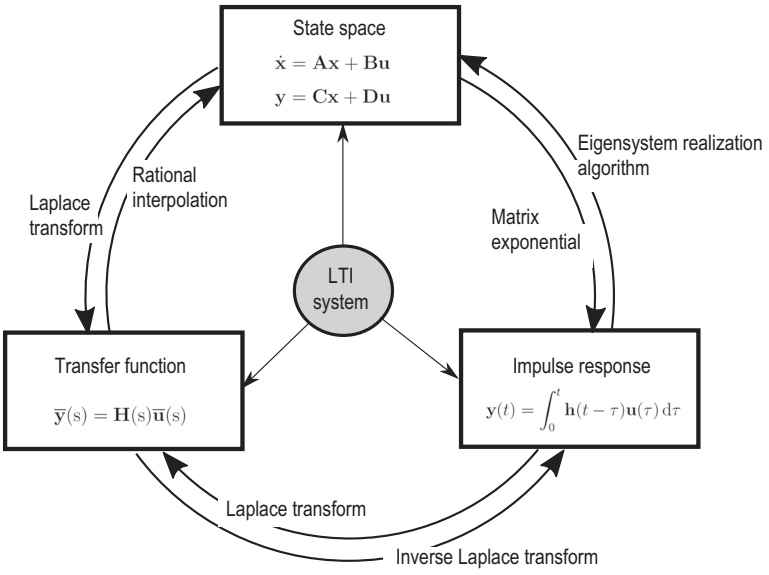

Figure 1.10 Three representations of linear time-invariant systems (after Brunton and Kutz (2019)).

representation, its transfer function, or its impulse response. They are schematically shown in Figure 1.10. As will be made apparent later, each one of them offers advantages over the other two for specific analyses. The rest of this section will discuss them, introducing the key definitions in each formulation, as well as the transformations to switch between any two of those three representations for a given system.

State-Space Representation

As we have seen in Section 1.4.1, finite-dimensional dynamical systems result in ordinary differential equations in time. After linearization about an equilibrium point, they can be written in a state-space form as

$$\begin{aligned} \dot{\mathbf{x}} &= \mathbf{A}\mathbf{x} + \mathbf{B}\mathbf{u}, \\ \mathbf{y} &= \mathbf{C}\mathbf{x} + \mathbf{D}\mathbf{u}, \end{aligned} \tag{1.5}$$

where $\mathbf{x}(t)$ is the state vector, of dimension N_x, and $\mathbf{A}$ is the $N_x \times N_x$ state matrix, $\mathbf{B}$ is the $N_x \times N_u$ input matrix, $\mathbf{C}$ is the $N_y \times N_x$ output matrix, and $\mathbf{D}$ is the $N_y \times N_u$ feedthrough matrix. For a given physical system, and input and output magnitudes of interest, the definition of the state vector is not unique, that is, there are multiple, but equivalent, realizations of Equation (1.5) for a given problem. In particular, a *minimal realization* is obtained when the system dynamics are described with the smallest possible number of states.[12]

[12] The formal definition is that the system realization has no uncontrollable and unobservable states (see Section 7.4 for further details).

https://doi.org/10.1017/9781108354868.002 Published online by Cambridge University Press

Once a suitable state vector is chosen, Equation (1.5) can be integrated in time for the given initial conditions $\mathbf{x}(0) = \mathbf{x}_0$ and the input signal $\mathbf{u}(t)$. Time-marching schemes, such as those of the Runge–Kutta family of algorithms, are readily available for this task.

Equation (1.5) is the continuous-time state-space representation of an LTI system. It is sometimes more suitable to write it as a *discrete-time system* in which all signals are only evaluated at sampling points with, typically, a constant sampling rate Δt. Let $\mathbf{x}_n = \mathbf{x}(t_n)$; with $t_n = n\Delta t$, the integration of Equation (1.5) between t_n and t_{n+1} results in the difference equations

$$\mathbf{x}_{n+1} = \hat{\mathbf{A}}\mathbf{x}_n + \hat{\mathbf{B}}\mathbf{u}_n, \tag{1.6}$$

with $\hat{\mathbf{A}} = e^{\mathbf{A}\Delta t}$ and $\hat{\mathbf{B}} = \int_0^{\Delta t} e^{\mathbf{A}\tau}\mathbf{B}\,\mathrm{d}\tau$, while the output equations remain unchanged. This is the *discrete-time state-space* representation of the system.

The state-space representation of an LTI system also allows establishing its linear (or asymptotic) stability from the eigenvalues of $\mathbf{A}$ or $\hat{\mathbf{A}}$, and its controllability and observability from the Gramians of the system, which are discussed in Section 7.4. To define linear stability, we study the response under small perturbations. They are introduced as the nonzero initial conditions $\mathbf{x}(0) = \mathbf{x}_0$ in Equation (1.5), and without forcing terms, that is, with $\mathbf{u} = \mathbf{0}$. A linear system is stable when it settles down to zero in its long-term response for any choice of $\mathbf{x}_0$. The solution of this problem can be directly obtained as

$$\mathbf{x}(t) = e^{\mathbf{A}t}\mathbf{x}_0, \tag{1.7}$$

where the *matrix exponential* of a matrix $\mathbf{A}$ is defined as

$$e^{\mathbf{A}} = \exp\mathbf{A} = \mathcal{I} + \sum_{n=1}^{\infty} \frac{\mathbf{A}^n}{n!}. \tag{1.8}$$

The evaluation of this series is in general something to be avoided, and for small systems that can be achieved by the use of the Cayley–Hamilton theorem (see Section 5.4.2). Alternatively, we can seek the solution by means of the modal projection of the system. For that, consider first the eigendecomposition

$$\mathbf{A}\boldsymbol{\Phi} = \boldsymbol{\Phi}\boldsymbol{\Lambda}, \tag{1.9}$$

where $\boldsymbol{\Lambda}$ is the diagonal matrix of, in general, the complex eigenvalues of $\mathbf{A}$ and $\boldsymbol{\Phi}$ is a matrix whose columns are its associated eigenmodes.[13] We introduce then the change of variable $\mathbf{x} = \boldsymbol{\Phi}\mathbf{z}$, which, for the unforced problem, results in the system dynamics written as $\dot{\mathbf{z}} = \boldsymbol{\Lambda}\mathbf{z}$. This equation can be integrated independently for each mode since $\boldsymbol{\Lambda}$ is diagonal, and this finally enables explicit solutions in the original variables to be obtained, thus resulting in

$$e^{\mathbf{A}t} = \boldsymbol{\Phi}e^{\boldsymbol{\Lambda}t}\boldsymbol{\Phi}^{-1}. \tag{1.10}$$

[13] This assumes that there are no repeated eigenvalues in the system; otherwise, we need the Jordan form of the eigendecomposition. This technical difference, however, effectively changes little in our discussion.

https://doi.org/10.1017/9781108354868.002 Published online by Cambridge University Press

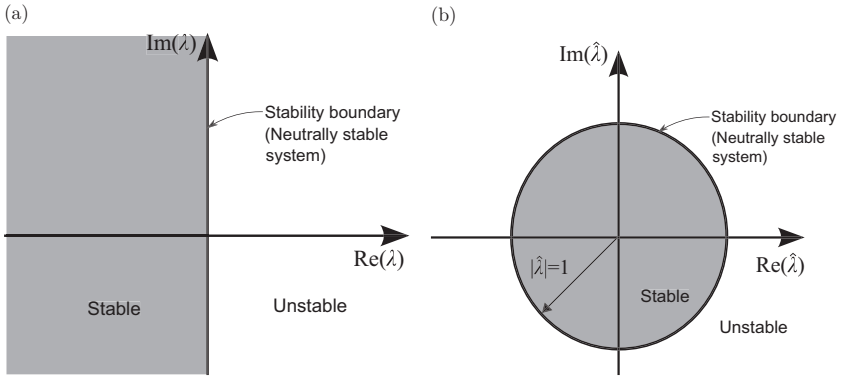

Figure 1.11 Asymptotic stability of linear time-invariant systems. (a) Continuous system, $\lambda = \text{eig}(\mathbf{A})$ and (b) discrete system, $\hat{\lambda} = \text{eig}(\hat{\mathbf{A}})$.

Since $\mathbf{\Phi}$ is a constant matrix, the solution to Equation (1.10) returns to zero as time grows if and only if all the eigenvalues of $\mathbf{A}$ are all in the left-half complex plane, as shown in Figure 1.11a. Finally, note that if λ is an eigenvalue of $\mathbf{A}$ in Equation (1.5), then $e^{\lambda \Delta t}$ is an eigenvalue of $\hat{\mathbf{A}}$ in Equation (1.6). Therefore, a discrete-time system is stable if and only if all the eigenvalues of $\hat{\mathbf{A}}$ are within the unit circle in the complex plane. This is graphically illustrated in Figure 1.11b.

Impulse Response

Given initial conditions $\mathbf{x}(0) = \mathbf{x}_0$, the solution to the state equation (1.5) can be obtained in terms of

$$\mathbf{x}(t) = e^{\mathbf{A}t}\mathbf{x}_0 + \int_0^t e^{\mathbf{A}(t-\tau)}\mathbf{B}\mathbf{u}(\tau)\,\mathrm{d}\tau. \tag{1.11}$$

Equation (1.11) is easily verified by substituting it into the differential equation (1.5). We say then that the exponential matrix $e^{\mathbf{A}(t-\tau)}$ is the *state-transition matrix* of the continuous-time LTI system. The output variable is finally obtained as

$$\mathbf{y}(t) = \mathbf{C}e^{\mathbf{A}t}\mathbf{x}_0 + \int_0^t \mathbf{C}e^{\mathbf{A}(t-\tau)}\mathbf{B}\mathbf{u}(\tau)\,\mathrm{d}\tau + \mathbf{D}\mathbf{u}(t). \tag{1.12}$$

We can now define the *impulse response* as the matrix function with the time history of the outputs to a unit impulse in the inputs, $\mathbf{u}(0) = \boldsymbol{\delta}(t)$, with $\boldsymbol{\delta}(t)$ being the Dirac delta function over an N_u-dimensional space. Thus, the impulse response, $\mathbf{h}(t)$, can be written as

$$\mathbf{h}(t) = \mathbf{C}e^{\mathbf{A}t}\mathbf{B} + \mathbf{D}\boldsymbol{\delta}(t). \tag{1.13}$$

The impulse response of a system is therefore a unique matrix function with time as the independent variable, which has N_y rows and N_u columns. Using this definition, the output signal for a system initially at rest ($\mathbf{x}_0 = \mathbf{0}$) can be written as a *convolution integral*,

$$\mathbf{y}(t) = \int_0^t \mathbf{h}(t-\tau)\mathbf{u}(\tau)\,\mathrm{d}\tau. \tag{1.14}$$

https://doi.org/10.1017/9781108354868.002 Published online by Cambridge University Press

For a discrete-time system, the impulse response results in the series $\mathbf{h}_0 = \mathbf{D}$ and $\mathbf{h}_n = \mathbf{C}e^{\mathbf{A}(n-1)\Delta t}\mathbf{B}$ for $n > 0$, which is known as the *Markov parameters* of Equation (1.6). The convolution operation can then be written as

$$\mathbf{y}_n = \sum_{m=1}^{n} \mathbf{h}_m \mathbf{u}_{n-m}, \quad \text{for} \quad n > 0, \tag{1.15}$$

and $\mathbf{y}_0 = \mathbf{h}_0\mathbf{u}_0$. Note that, as they are instantiations of the impulse response, the Markov parameters are matrices whose number of rows and columns are the number of outputs and inputs, respectively. As has just been seen, the evaluation of the impulse response from a state-space model (the differential equations describing the system dynamics) is a straightforward process. The converse, that is, effortlessly obtaining a state-space description from either an impulse response or Markov parameters is generally not true, and it becomes a form of the realization problem that we discuss in Section 1.4.3.

Transfer Function

Finally, it is often convenient to study the dynamics of a system in the frequency domain. The Laplace transform gives a generic tool to enable that transformation. For a time-domain function $g(t)$, its Laplace transform, $\overline{g}(\mathrm{s})$, is defined as

$$\overline{g}(\mathrm{s}) = \int_0^\infty g(t)e^{-\mathrm{s}t}\mathrm{d}t, \tag{1.16}$$

where s is a complex variable known as the Laplace variable. A major advantage of Equation (1.16) is that it transforms differential equations into algebraic equations, since it is easy to see that the Laplace transform of $\frac{\mathrm{d}}{\mathrm{d}t}g(t)$ is $g(0) + \mathrm{s}\overline{g}(\mathrm{s})$. Considering now the LTI system given by Eq. (2.19) with zero initial conditions, its Laplace transform results in

$$\begin{aligned} \mathrm{s}\overline{\mathbf{x}}(\mathrm{s}) &= \mathbf{A}\overline{\mathbf{x}}(\mathrm{s}) + \mathbf{B}\overline{\mathbf{u}}(\mathrm{s}), \\ \overline{\mathbf{y}}(\mathrm{s}) &= \mathbf{C}\overline{\mathbf{x}}(\mathrm{s}) + \mathbf{D}\overline{\mathbf{u}}(\mathrm{s}), \end{aligned} \tag{1.17}$$

where $\overline{\mathbf{u}}(\mathrm{s})$ and $\overline{\mathbf{y}}(\mathrm{s})$ are the Laplace transforms of the input and output vectors, respectively. It is possible to solve $\overline{\mathbf{x}}(\mathrm{s})$ in the first equation and substitute in the second, which results in a closed-form relation between inputs and outputs in the Laplace domain $\overline{\mathbf{y}}(\mathrm{s}) = \mathbf{H}(\mathrm{s})\overline{\mathbf{u}}(\mathrm{s})$. Here we have introduced the $N_y \times N_u$ matrix $\mathbf{H}(\mathrm{s})$ as the system *transfer function*

$$\mathbf{H}(\mathrm{s}) = \mathbf{C}\left(\mathrm{s}\boldsymbol{\mathcal{I}} - \mathbf{A}\right)^{-1}\mathbf{B} + \mathbf{D}. \tag{1.18}$$

Stable linear systems, which have been defined above, can additionally be studied in the frequency domain. This is the restriction of the Laplace domain to the imaginary axis, that is, $\mathrm{s} = \mathrm{i}\omega$, which results in the *frequency-response function* (FRF) of the system

$$\mathbf{H}(\mathrm{i}\omega) = \mathbf{C}\left(\mathrm{i}\omega\boldsymbol{\mathcal{I}} - \mathbf{A}\right)^{-1}\mathbf{B} + \mathbf{D}. \tag{1.19}$$

The FRF can be determined, both experimentally and numerically, by exciting the system with harmonic inputs at the frequencies of interest and considering the

https://doi.org/10.1017/9781108354868.002 Published online by Cambridge University Press

steady-state response in the outputs after the initial transient dynamics have dissipated (thus the condition of asymptotic stability). In mechanical systems, the FRF is also referred to as *admittance*.

Replacing the complex-valued Laplace variable in the Laplace transform by $\mathrm{i}\omega$ defines the Fourier transform for continuous-time systems, and the Z-transform for discrete-time ones. Both transformations are discussed in some detail in Appendix A. In particular, Equation (A.8) derives the Fourier transform of the convolution integral, which has been introduced in Equation (1.14). From that, it can be seen that the FRF of a linear system is the Fourier transform of its impulse response (scaled by a factor of 2π), that is,

$$\mathbf{H}(\mathrm{i}\omega) = \int_{-\infty}^{\infty} \mathbf{h}(t) e^{-\mathrm{i}\omega t}\, \mathrm{d}t. \tag{1.20}$$

We have by now identified the transformations that define the FRF of a system from either its state-space representation, Equation (1.19), or its impulse response description, Equation (1.20). The impulse response is equally obtained from the inverse Fourier transform of the FRF; yet, the general problem of obtaining the state-space realization of a system given by its frequency-response or its transfer function can only be solved approximately (see Section 1.4.3). An important exception to this occurs when $\mathbf{H}(\mathrm{s})$ is given by proper rational entries, that is, when the transfer function can be written as

$$\mathbf{H}(\mathrm{s}) = \mathbf{D} + \frac{1}{\mathbf{r}(\mathrm{s})}\mathbf{P}(\mathrm{s}), \tag{1.21}$$

where $\mathbf{r}(\mathrm{s}) = s^n + \sum_{k=0}^{n-1} \mathrm{s}^k r_k$ is a polynomial expression of order n with real coefficients r_k, and $\mathbf{P}(\mathrm{s}) = \sum_{k=0}^{n-1} \mathrm{s}^k \mathbf{P}_k$ is a matrix of polynomials of, at most, order $n-1$. The roots of $\mathbf{r}(\mathrm{s})$ are the poles of the system, while the roots of $\mathbf{P}(\mathrm{s})$ are the zeros of each input/output pair. The linear stability of the system corresponds to all poles being in the left-hand complex plane. When the zeros are also in the left-hand plane, the system is known as *minimum-phase system*. In such a case, the inverse system is also stable and unique, and therefore it is possible to determine uniquely its inputs from its outputs. Minimum-phase systems are causal, that is, their current outputs only depend on past and current inputs. In fact, an LTI system is minimum-phase if and only if the system and its inverse both are stable and causal.

A state-space realization for a system such as that of Equation (1.21) can be obtained with

$$\mathbf{A} = \begin{bmatrix} \mathbf{0} & \mathcal{I} & \mathbf{0} & \cdots & \mathbf{0} \\ \mathbf{0} & \mathbf{0} & \mathcal{I} & \cdots & \mathbf{0} \\ \vdots & \vdots & \vdots & \ddots & \vdots \\ \mathbf{0} & \mathbf{0} & \mathbf{0} & \cdots & \mathcal{I} \\ -r_0\mathcal{I} & -r_1\mathcal{I} & -r_2\mathcal{I} & \cdots & -r_{n-1}\mathcal{I} \end{bmatrix}, \quad \mathbf{B} = \begin{bmatrix} \mathbf{0} \\ \mathbf{0} \\ \cdots \\ \mathbf{0} \\ \mathcal{I} \end{bmatrix},$$
$$\mathbf{C} = \begin{bmatrix} \mathbf{P}_0 & \mathbf{P}_1 & \mathbf{P}_2 & \cdots & \mathbf{P}_{n-1} \end{bmatrix}, \tag{1.22}$$

https://doi.org/10.1017/9781108354868.002 Published online by Cambridge University Press

as well as the feedthrough matrix $\mathbf{D}$, that was already introduced in Equation (1.21). All the block matrices in Equation (1.22) have the same dimensions as $\mathbf{H}$. This realization however may not be minimal, thus benefiting from additional model-order reduction strategies to remove unnecessary internal dynamics. Reduced-order model (ROM) generation is discussed in this book in Section 7.4 in the context of unsteady aerodynamics.

Example 1.1 Flapped Airfoil with Vertical Displacements in a Horizontal Flow. Consider the moving airfoil of a chord c and a unit span as shown in Figure 1.12. The airfoil has mass m, and it is suspended by a spring k_h; therefore, when in vacuum, it is a spring-mass mechanical system with natural frequency $\omega_h = \sqrt{\frac{k_h}{m}}$. It is then positioned in a horizontal airstream with velocity V and density ρ and actuated by a flap. In the first approximation, the flap generates lift proportional to its deflection, $\beta(t)$, while the motions of the airfoil generate lift proportional to the effective angle of attack $\dot{h}/V$. As a result, the equation of motion for $V > 0$ of the resulting aeroelastic system can be written as

$$m\ddot{h} + k_h h = -\frac{1}{2}\rho V^2 c \left(c_{l_\alpha} \frac{\dot{h}}{V} + c_{l_\beta} \beta \right). \tag{1.23}$$

The right-hand side in this equation is the instantaneous lift per unit span on the airfoil, which appears with a negative sign due to the sign convention in the definition of the vertical coordinate, $h(t)$ (see Figure 1.12). We can rewrite it as

$$\ddot{h} + \left(\mu_\alpha / V\right) \dot{h} + \omega_h^2 h = -\mu_\beta \beta, \tag{1.24}$$

where we have defined $\mu_\bullet = \frac{\rho V^2 c c_{l_\bullet}}{2m} > 0$. This can be written in a state-space form by defining the state vector $\mathbf{x}^\top = \left\{ h \quad \dot{h} \right\}$, input $u = \beta$, and choosing an output of interest, for example, $y = h$. This results in the dynamics written as Equation (1.5), with

$$\mathbf{A} = \begin{bmatrix} 0 & 1 \\ -\omega_h^2 & -\mu_\alpha / V \end{bmatrix}, \qquad \mathbf{B} = \begin{Bmatrix} 0 \\ -\mu_\beta \end{Bmatrix}, \qquad \mathbf{C} = \begin{Bmatrix} 1 & 0 \end{Bmatrix}. \tag{1.25}$$

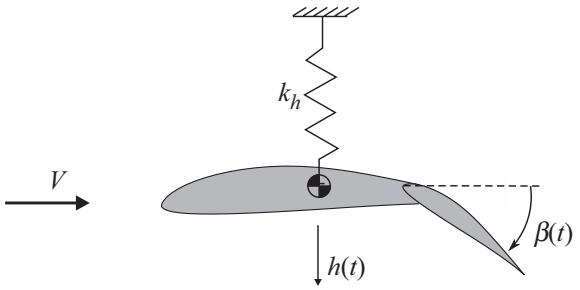

Figure 1.12 Airfoil with a trailing-edge flap suspended by a vertical spring.

https://doi.org/10.1017/9781108354868.002 Published online by Cambridge University Press

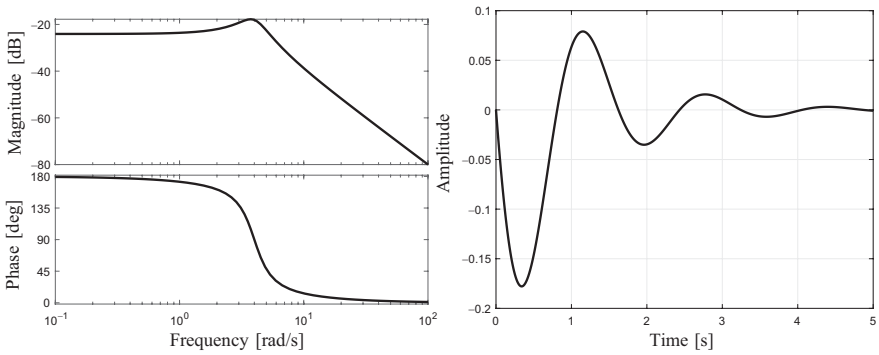

Figure 1.13 Frequency response function, $H(\mathrm{i}\omega)$, and impulse response, $h(t)$, for $\mu_\alpha/V = 2$, $\mu_\beta = 1$, and $\omega_h = 4$. (a) Bode plot and (b) impulse response.

For zero initial conditions, applying the Laplace transform to Equation (1.24) results in

$$\left(\mathrm{s}^2 + \left(\mu_\alpha/V\right)\mathrm{s} + \omega_h^2\right)\overline{h}(\mathrm{s}) = -\mu_\beta\overline{\beta}(\mathrm{s}), \tag{1.26}$$

which defines the following (scalar) transfer function for the single-input–single-output system

$$H(\mathrm{s}) = \frac{\overline{h}(\mathrm{s})}{\overline{\beta}(\mathrm{s})} = -\frac{\mu_\beta}{\mathrm{s}^2 + \left(\mu_\alpha/V\right)\mathrm{s} + \omega_h^2}. \tag{1.27}$$

The FRF is then directly obtained from the restriction of Equation (1.27) to the imaginary axis, that is, $H(\mathrm{i}\omega)$. Finally, the impulse response function can be obtained from either the inverse Laplace transform of Equation (1.27) or from an analytical solution of Equation (1.24), with $u = \delta(t)$ being the Dirac delta function. In either case, it results in

$$h(t) = -\frac{\mu_\beta}{\omega_h\sqrt{1-\zeta^2}}e^{-\zeta\omega_h t}\sin\left(\sqrt{1-\zeta^2}\omega_h t\right), \tag{1.28}$$

with $\zeta = \frac{\mu_\alpha}{2V\omega_h}$. Figure 1.13a shows the amplitude and phase of the FRF in log–log scale (known as the *Bode plot*) for $\mu_\alpha/V = 2$, $\mu_\beta = 1$, and $\omega_h = 4$, while Figure 1.13b shows the corresponding impulse response function. This simple aeroelastic system is a damped oscillator, with the damping generated from the aerodynamic forces.

1.4.3 Dynamical System Identification

In the previous section, we have discussed three equivalent representations of LTI systems. The first of them, the state-space model, uses inputs, states, and outputs, while the last two, namely the impulse response and the transfer function descriptions, only use inputs and outputs. Consequently, the state-space representation is often referred to as the *internal* description, while the other two (which are a Laplace/Fourier transform pair) are known as *external* descriptions (Antoulas, 2005, Ch. 4). We have seen that the

https://doi.org/10.1017/9781108354868.002 Published online by Cambridge University Press

transformation from internal to external descriptions is obtained from direct manipulation of the system matrices $(\mathbf{A}, \mathbf{B}, \mathbf{C}, \mathbf{D})$. The inverse problem, that is, obtaining an internal description from an external one, is in general significantly more involved, and it is known as the *realization problem*. Moreover, in most practical applications, input/output information is only available either at discrete times or for a finite range of frequencies and, therefore, the realization problem can only be approximately solved. In fact, it becomes a data-driven system identification problem, with the data being a finite number (at sampled frequencies or times) of input/output pairs of the dynamical system. The literature on system identification methods is vast, and here we focus on two methods of particular importance to unsteady aerodynamics, namely the eigensystem realization algorithm (ERA) and rational interpolation methods, which will be used later in this book.

Eigensystem Realization Algorithm

The ERA builds a state-space representation of a given dynamical system from its impulse response, which may have been obtained either experimentally or numerically. As the data series are necessarily finite, the approach works in discrete time and generates the internal model from a finite series of Markov parameters, Equation (1.15). It has been extensively used to analyze experimental vibration, for which it was originally developed (Juang and Pappa, 1985), and to construct low-order models from (expensive) computational fluid-dynamics simulations (Silva and Bartels, 2004), which are discussed in Section 6.5.4.

The ERA seeks to identify the dominant underlying features in the data series. For that purpose, it starts by building a rectangular matrix with all the output measurements to the impulse response, which are shifted by one time step on each column, as

$$\mathcal{H}_k = \begin{bmatrix} \mathbf{h}_{k+1} & \mathbf{h}_{k+2} & \cdots & \mathbf{h}_{k+N} \\ \mathbf{h}_{k+2} & \mathbf{h}_{k+3} & \cdots & \mathbf{h}_{k+N+1} \\ \vdots & \vdots & \ddots & \vdots \\ \mathbf{h}_{k+M} & \mathbf{h}_{k+M+1} & \cdots & \mathbf{h}_{k+N+M-1} \end{bmatrix}. \tag{1.29}$$

This is known as the truncated *Hankel matrix* for the system at the reference time t_k. Here, M defines the time window where the dynamics of interest occur, which are normally determined in terms of frequency bandwidth. The number of columns, N, determines the number of measurements used to extract the dominant temporal patterns. As a result, $N+M-1$ time samples are needed to populate the Hankel matrix. Their dominant features are then extracted from a singular value decomposition (SVD) with reference to the origin of times, $k=0$, that is,

$$\mathcal{H}_0 = \mathbf{U}\boldsymbol{\Sigma}\mathbf{V}^\top, \tag{1.30}$$

where $\boldsymbol{\Sigma}$ is the diagonal matrix of the (real and nonnegative) singular values, and $\mathbf{U}$ and $\mathbf{V}$ are real orthogonal matrices whose columns are the left and right singular vectors, respectively. The SVD is the essential algorithm in modern data-driven methods (Brunton and Kutz, 2019, Ch. 1), as it enables the reduction of high-dimensional datasets into low-order approximations. To achieve this, the SVD representation is

https://doi.org/10.1017/9781108354868.002 Published online by Cambridge University Press

partitioned such that only the largest singular values are retained. Let $\hat{\mathbf{\Sigma}}$ be the resulting truncated set of singular values. Since it is a diagonal matrix, it is easy to see that only the corresponding singular vectors need to be retained in a truncated approximation. This results in very narrow matrices $\hat{\mathbf{U}}$ and $\hat{\mathbf{V}}$ that approximate the Hankel matrix as $\mathcal{H}_0 \approx \hat{\mathbf{U}}\hat{\mathbf{\Sigma}}\hat{\mathbf{V}}^\top$. Finally, it can be shown (Juang and Pappa, 1985) that a low-order discrete-time state-space model of the system can be constructed from the SVD as

$$\begin{aligned}
\hat{\mathbf{A}} &= \hat{\mathbf{\Sigma}}^{-1/2}\hat{\mathbf{U}}^\top \mathcal{H}_1 \hat{\mathbf{V}}\hat{\mathbf{\Sigma}}^{-1/2}, \\
\hat{\mathbf{B}} &= \hat{\mathbf{\Sigma}}^{1/2}\hat{\mathbf{V}}^\top \begin{bmatrix} \mathcal{I}_u \\ \mathbf{0} \end{bmatrix}, \\
\hat{\mathbf{C}} &= \begin{bmatrix} \mathcal{I}_y & \mathbf{0} \end{bmatrix} \hat{\mathbf{U}}\hat{\mathbf{\Sigma}}^{1/2}, \\
\hat{\mathbf{D}} &= \mathbf{0},
\end{aligned} \tag{1.31}$$

where $\mathcal{I}_u$ and $\mathcal{I}_y$ are unit matrices whose dimension is the number of inputs and outputs, respectively.

Rational Interpolation

Rational interpolation methods build a state-space model from a sampled transfer function. They are therefore the frequency domain equivalent to the ERA considered above. In a similar manner to the Hankel matrix for the time-domain problem, a matrix of sampled frequency-domain data, known as the Löwner matrix, can be assembled (Mayo and Antoulas, 2007) and used in conjunction with a truncated SVD to derive a low-order internal model. This approach has been recently explored by Yue and Zhao (2020) and Quero et al. (2021) to obtain an elegant process of system identification from frequency-domain unsteady aerodynamics datasets.

In this book, however, we will restrict ourselves to the well-established approach used in aeroelasticity, known as the *rational-function approximation*. Here, an Ansatz is chosen for the FRF of the system (e.g., a structure such as Equation (1.19) with a diagonal state matrix), whose coefficients are then obtained by least-squares fitting on the sampled data. The resulting description is finally expanded to the full complex plane using analytical continuation. Further details of this method are discussed in Section 6.5.3.

1.5 Outline of This Book

This chapter has laid the groundwork for this book. We have seen that it comes in response to both some long-term trends in aircraft design to build vehicles with increasingly dominant aeroelastic effects and the more short-term disruptions associated with the search for zero-emission solutions to mitigate climate change. Our interest throughout is on the dynamics of air vehicles, and consequently, the book makes the extensive use of the standard analysis methods for dynamical systems

https://doi.org/10.1017/9781108354868.002 Published online by Cambridge University Press

throughout. The readers are expected to be familiar with state-space equations, transfer functions, and Fourier transforms. A basic introduction has been included in this chapter, and some additional material can be found in the appendices. A more detailed description of some other, more specific, mathematical tools of relevance to the analysis of the flexible aircraft dynamics is inserted throughout the book.

The rest of the material in this book has been structured into 10 additional chapters that collectively build a rather generic framework for modeling, simulation, and control of flexible aircraft. A consistent notation is used throughout; yet most chapters are also self-contained to enable readers to focus on specific topics. As we are often concerned here with flight in a nonstationary atmosphere, an overview of the most relevant atmospheric conditions for aircraft design is first introduced in Chapter 2. The main results of that chapter are later used in subsequent chapters to investigate the dynamic response of both the rigid and flexible air vehicles.

Chapter 3 is mostly a self-contained introduction to the problems in unsteady aerodynamics and aeroelasticity that are relevant to this book, including dynamic stability and response to atmospheric gusts. It introduces those concepts using the analytical solutions for thin airfoils of Theodorsen and Sears, which serve to build time-domain formulations of the simple aeroelastic systems and their response to atmospheric disturbances. It can be used as the basis on a short introductory course to aeroelasticity.

Chapter 4 reviews the equations of motion that describe the flight dynamics of rigid aircraft. As a characteristic feature of this book, this is done in the context of flight in a nonsteady atmosphere, with still-air conditions presented as a particular case. The general Newton–Euler equations of motions for the rigid body are derived for an aircraft with arbitrary kinematics, as well as the linearized solutions for the longitudinal and lateral problems, which are written in a state-space form. Linear quasi-steady aerodynamics is used, with the stability and control derivatives assembled into matrices of aerodynamic influence coefficients. The material is self-contained and can serve as a brief course in flight mechanics. It also introduces both inertial and body-attached reference frames that are needed again in later chapters to describe the unsteady aerodynamics and the flexible aircraft dynamics, respectively.

The effect of flexibility on the aircraft dynamics is first introduced in Chapter 5 under certain restrictive assumptions that will be systematically removed in the following chapters. In particular, Chapter 5 considers flight dynamics for the case in which there is a sufficient frequency separation between the rigid-body and the vibration characteristics of the aircraft. This situation occurs in many aircraft over a large portion of its flight and maneuvering envelope and results in the so-called elastified equations of motion. In that solution, the degrees of freedom are still those describing the rigid-body kinematics of the aircraft but with modified coefficients that account for the aeroelastic effects. This formulation is also generally valid for most static problems and is therefore used to introduce aeroelastic trim and control reversal.

A more general description is needed when the elastic deformations have a nonnegligible effect of on the inertia of the vehicle, and this will be the focus of Chapter 6. The assumption in this chapter is of small-amplitude vibrations, in which case the vehicle dynamics can be written in a compact form in modal coordinates. Consequently, we

will define linear normal modes in structural dynamics and use them to project the general equations of motion of a flexible unsupported body. As we consider a larger frequency space, unsteady aerodynamics need to be considered. The focus is on the nonstationary aerodynamic forces resulting from the small-amplitude wall motions, which are obtained from applying the data-driven system identification techniques of Section 1.4.3 to suitable fluid-dynamics models. This defines the generalized aerodynamic forces associated with the modal description from results obtained from either computational fluid dynamics (using ERA) or potential flow aerodynamics (using rational interpolation). Many of the aeroelastic and flight dynamics concepts first introduced in Chapter 3 and Chapter 4, respectively, are revisited for flexible aircraft displaying dynamic couplings between its rigid and flexible modes.

While there is a restriction on the amplitude of elastic deformations in Chapter 6, the aerodynamic models are generally valid for subsonic and transonic flight. Subsequent chapters deal with arbitrary large wing deformations, although still with attached flows, as the interest is enabling deformation to achieve structural efficiency. They will, however, assume an incompressible flow regime, as most vehicles currently displaying large deformations fly at low speed. Chapter 7 reviews time-domain unsteady aerodynamic models for such conditions, with a particular focus on the unsteady vortex-lattice method. As in the previous chapter, the interest in this chapter is on the aerodynamic forces resulting from the motions of the structure, and the high computational cost of evaluating them on the general approach is lowered by considering reduced-order modeling techniques, in particular, balanced realizations of the aerodynamic equations.

The structural models for aircraft with large elastic deformations are considered in Chapter 8. As before, we restrict ourselves to a commonly found strategy that is suitable for most aircraft displaying geometric nonlinearity. In particular, the chapter presents several flexible multibody dynamic modeling approaches based on geometrically nonlinear composite beams. The mean assumption of a beam model is that the structural dynamics can be well approximated by tracking a reference line with suitable stiffness and inertial properties. In the case of composite beams, that description also allows elastic couplings between the different degrees of freedom (e.g., coupling between the bending and torsion of the wing). Three alternative solutions to the beam equations are presented, namely a conventional finite-element model based on nodal displacement and rotations and two alternative methods that use spatial and time derivatives of the displacement field as primary variables. They enable different analysis techniques for very flexible aircraft in the final chapters and are therefore jointly presented.

Chapter 9 combines the unsteady aerodynamic models of Chapter 7 and the composite beams models of Chapter 8 to describe the dynamics of very flexible aircraft. This approach naturally captures the nonlinear couplings between flight dynamics and the aeroelastic response of the vehicle, including the expense of a higher computational time. To address that, we include an approximated solution method on the basis of the modal projection of the nonlinear equations and linearized aerodynamics, which hugely reduces the computational burden on the simulation. Next, typical situations

https://doi.org/10.1017/9781108354868.002 Published online by Cambridge University Press

are exemplified using numerical results on several recent prototypes that were purposely built to explore geometric nonlinearities in highly efficient wings and aircraft. Finally, the chapter reviews some analysis methods in aircraft design that are strongly affected by airframe deformations (static and dynamic stability, loads, flight control, etc.) and suggests methodological improvements to accommodate the more complex physics associated with increased flexibility.

Feedback control is then considered in Chapter 10. Even though we make extensive use of methods and language of control theory throughout this book, all the previous chapters to Chapter 10 consider the open-loop dynamics of the aircraft. Here, we introduce first the common elements to a control architecture for flexible aircraft, and the focus is then on optimal control methods to determine a suitable logic. Both linear and nonlinear methods are outlined, with examples and applications in aeroelasticity and the flexible aircraft dynamics. The methodological sections of the chapter start with a summary of the linear quadratic regulator, for which some details of the solution process using Lagrange multipliers are included. That is then expanded to the nonlinear problem, which is formulated within the paradigm of model predictive control, with an efficient internal model derived in Chapter 9. Equally, the estimation problem, that is, the approximate reconstruction of the state from limited measurements is first presented for linear problems, with a discussion on Kalman filters. This is finally expanded to a nonlinear problem with an outline of the moving-horizon estimator. The strong connections between the optimal control and estimation problems for both linear and nonlinear problems are highlighted.

Finally, Chapter 11 outlines the current industrial methods for experimental modal analysis of air vehicles. Both ground and flight vibration tests are discussed, with a focus on large transport aircraft with moderately flexible wings.

https://doi.org/10.1017/9781108354868.002 Published online by Cambridge University Press